



COMPUTATIONAL ELECTROMAGNETIC TECHNIQUE FOR BROADBAND  
ANALYSIS OF MICROSTRIP ANTENNAS

<sup>1</sup>M.A. Mangoud, <sup>2</sup>R.A. Abd-Alhameed, <sup>2</sup>P.S. Excell and <sup>1</sup>M. Aboul-Dahab  
<sup>1</sup>Arab Academy for Science and Technology, Egypt. <sup>2</sup>University of Bradford, UK

**Abstract:** Broadband analysis of a microstrip patch antenna on a finite substrate is investigated using the Finite Difference Time Domain (FDTD) method. The effects of varying the ground and dielectric size against the return loss at the input port and the far fields are discussed. Two different ways of feeding the antenna are addressed. The problem space size requirements of the FDTD method are presented. A thin wire code that includes the wire radius of the coaxial feed cable is used. The frequency response of several microstrip patch antennas is analysed over wide bandwidths, using Gaussian pulses with a total bandwidth of 20GHz. The results are in good agreement with measurements.

## 1. INTRODUCTION

Many of the numerous papers and textbooks dealing with the analysis of microstrip antennas utilise some form of approximation. The most accurate analytical technique uses the familiar Sommerfeld formulation [1]. The drawback of this approach, however, is the inherent inability to handle finite microstrip substrate structures. Methods to overcome this problem include frequency-domain methods using surface/surface and volume/surface formulations [2,3] or time-domain methods, for example the Finite-Difference Time-Domain numerical technique (FDTD) [4]. The latter has some significant advantages since the frequency-domain methods require substantial amounts of memory and they have difficulties in modelling multi-layer antenna substrates. Many authors have used this technique, using one side of the perfectly matched layer (PML) boundary [5,6] to represent the dielectric and the ground plane of the finite size microstrip patch antenna. This causes some difficulties in computing near and far fields from the radiating system.

In this paper, the finite geometry of the antenna is simulated inside the FDTD problem space. In this way the effects of the finite size of both the dielectric and the ground can be investigated and discussed separately and their effect on the behaviour of the near/far fields and the return loss at the input ports investigated. The antenna feed network, using a coaxial cable or a stripline is also studied. The method uses a thin wire code to include the effect of the wire radius of the coaxial feed [7]. The frequency response of the antenna is analysed over an instantaneous broad bandwidth by driving with a Gaussian pulse of entire bandwidth 20GHz. The number of time steps is reduced by introducing internal impedance into the source, even though the dielectric is considered lossless [8]. Two patch antennas were analysed and fabricated and the results compared with measurements. The results of the proposed method show good agreement with the measurements.

## 2. FORMULATION OF THE METHOD

The finite difference time domain (FDTD) method has become an increasingly popular approach for analysing the electromagnetic performance of antennas and microstrip devices. With transient excitation, it provides impedance and scattering parameters over a wide frequency band from one calculation plus application of the discrete Fourier transform (DFT). The application of the method to microstrip patch antennas can be classified as follows:



## 2.1. Excitation Treatment

Microstrip lines and coaxial probes are the basic structures used to feed the patch antennas. The Gaussian pulse is used as the source of excitation because of its smooth Gaussian-shape spectrum, which can provide information from dc to the desired frequency, simply by adjusting the width of the pulse. In the case of a patch fed by a microstrip line, the electric or magnetic wall conditions are used at the radiating boundaries of the device [5], i.e. at the points at which the wave is launched. The excitation pulse of vertical electric field is applied underneath the microstrip line. This pulse represents a fictitious source whose field will be forced by the boundary condition to take on a realistic distribution after the wave propagates a distance of a few FDTD lattices [9]. The parameters of the excitation Gaussian pulse and its Fourier transform can be stated respectively as follows:

$$v(t) = Ae^{-g^2(t-t_0)^2} \quad (1)$$

$$\text{and } v(j\omega) = -A \frac{\sqrt{\pi}}{g} e^{-j\omega t_0} e^{-(\omega/4g)^2} \quad (2)$$

where A is the amplitude, g is the inverse rise time and  $t_0$  is the time delay. The values that will be used through the present work, giving approximately 20GHz entire bandwidth, are:  $A = 1V$ ;  $g = 1/15e^9s^{-1}$  and  $t_0 = 3/g$  s. For these particular values, the pulse and its corresponding spectrum and phase are shown in Fig. 1.

## 2.2. Cell size and time step

The choice of cell size is critical in applying FDTD. It must be small enough to permit accurate results at the highest frequency of interest, and yet be large enough to keep the resource requirement manageable. Cell size is directly affected by the penetrable media present. The greater the permittivity or conductivity, the shorter the wavelength at a given frequency and the smaller the cell size required. The fundamental constraint is that the cell size must match the smallest wavelength for which accurate results are desired. From the Nyquist sampling theorem, there must be at least two samples per spatial period (wavelength) in order for the spatial information to be adequately sampled. Because the sampling is not exact and the wavelength is not precisely determined, more than two samples per wavelength are required [2]. Thus, the length of longest edge of the cell (ds) for good results can be expressed as:

$$ds \leq \frac{\lambda}{20\sqrt{\epsilon_r}} \quad (3)$$

where  $\lambda$  is the free space wavelength and  $\epsilon_r$  is the relative permittivity of the medium. The time step ( $\Delta t$ ) for given cell dimensions is required to be:

$$\Delta t \leq \frac{1}{c \sqrt{\frac{1}{\Delta x^2} + \frac{1}{\Delta y^2} + \frac{1}{\Delta z^2}}} \quad (4)$$

where c is the velocity of light.  $\Delta x$ ,  $\Delta y$  and  $\Delta z$  are the rectangular cell side lengths.

## 2.3. Computation of S-Parameters using FDTD

The FDTD method was used to measure the S-parameters of the different microstrip antennas. Different approaches to obtain the S-parameters have been presented in the literature [5,6]. These discuss approaches intended to match the ports of a microstrip circuit with a lumped resistor model. These approaches require the FDTD construction of a fictitious load to terminate the ports of the structure, which is inconvenient when different cell sizes are desired to analyse the same problem. In the present work, the field difference equation around the source was updated following the same procedure as used in ref. [10]. This method implements a source with internal



impedance  $Z_s$  (normally  $50\Omega$ ). If the input voltage is represented by  $v_i(t)$  (usually the Gaussian pulse) and the impressed field is denoted by  $E_i$  inside the problem space, then, using the Kirchoff voltage law,  $E_i$  is given by:

$$E_i = v_i / ds - I_i Z_s / ds \quad (5)$$

where  $ds$  is the cell side in the direction of  $E_i$ .  $I_i$  (input current) can be computed using Ampere's law thus:

$$I_i = (H_x(i, j-1, k) - H_x(i, j, k))\Delta x + (H_y(i, j, k) - H_y(i-1, j, k))\Delta y \quad (6)$$

where  $i, j, k$  are the cell number indices of the excitation source field that is oriented in the direction of the  $z$ -axis. Thus, the input impressed field ( $E_i$ ) can be simply expressed using Eqns. 5 and 6 inside the FDTD problem space. Hence, the input impedance of the one-port network can be given by:

$$Z_i(j\omega) = \frac{-E_i(j\omega)\Delta z}{I_i(j\omega)} \quad (7)$$

Where  $E_i(j\omega)$  and  $I_i(j\omega)$  are the discrete Fourier transform (DFT) of the time domain signals of  $E_i(t)$  and  $I_i(t)$  respectively. The return loss for this port is computed using the following expression,

$$\text{Return loss} = 20 \log_{10} | S_{11}(j\omega) |, \quad \text{where} \quad S_{11}(j\omega) = \frac{Z_i(j\omega) - Z_o}{Z_i(j\omega) + Z_o} \quad (8)$$

and  $Z_o$  is the characteristic impedance, taken to be  $50\Omega$ .

## 2.4. Problem Space Set-Up

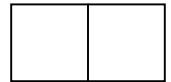
Once the time steps and the cell sizes have been calculated corresponding to the geometry of the antenna and the operating bandwidth, the complete problem space can be specified by including the PML. A few cells to represent the distance required from the PML in order to compute the far fields. This model was applied both to predict the forward radiation and also the backscattered field under the ground plane. Because the antenna structure is considered in the presence of finite dielectric and a finite ground plane it is a more accurate model than infinite-substrate versions. The structure is spaced away from the PML by 5 to 10 cells, in the centre of which was placed the equivalence-principle surface required to compute the far fields.

## 3. COMPUTED AND EXPERIMENTAL RESULTS

Three different microstrip patch antenna structures have been experimentally set-up in this work:

a,b. Circular patch and rectangular patch both fed by coaxial line. c. Rectangular patch fed by stripline.

These patches were constructed on 'Duroid' substrates with  $\epsilon_r = 2.55$ , thickness  $1.524\text{mm}$  and  $\tan \delta = 0.0018$ . The substrate parameters were constant over the entire bandwidth of the Gaussian pulse considered in Sect. 2.1. The width and length of the rectangular microstrip patches were  $18.9\text{mm}$  and  $23.1\text{mm}$  respectively. For the coaxial feed the feedpoint was placed  $4.8\text{mm}$  from the centre of the patch on the central axis parallel to its shorter sides. For the stripline feed, the stripline is in turn fed by a coaxial line at its free end. The radius of the coaxial centre conductor for both methods of feeding the rectangular patch was chosen to be  $0.41\text{mm}$ . The width and the length of the stripline were 5cells ( $1.5\text{mm}$ ) and 15cells ( $4.5\text{mm}$ ) respectively. The diameter of the circular patch was set to be  $20\text{mm}$  with the feedpoint placed 16cells ( $4.8\text{mm}$ ) from its centre. The size of the ground plane used was  $33.9 \times 33.9\text{mm}$ , equivalent to  $112 \times 112$  cells. The dielectric size was  $112 \times 112 \times 5$  cells, giving 5 cells to model the vertical field component inside the dielectric. The dielectric properties applying for the field components lying on the cell surfaces between the dielectric and free space were averaged to satisfy the boundary conditions. The separation distance between the PML and the antenna structure was taken to be 8 cells with the equivalence-principle surface placed in its centre. Finally, the PML layer was made 6 cells wide. The results are summarised below.



The computed input voltage and current at the input port of the coaxially-fed rectangular patch antenna are shown in Figs. 2 and 3 respectively. It is observed that the input voltage and current decayed as the time increased. This proves that the method is stable and the steady state can be reached with approximately 4000 time steps.

The spatial distribution of  $E_z$  just beneath the patch at 200, 400, 600 and 800 time steps is shown in Fig. 4, where the source Gaussian pulse and subsequent field propagation on the antenna are observed. The characteristic features of the propagation are also observed including enhancement of the field near the edges of the antenna geometry. The calculated and measured return loss at the input ports of stripline-fed rectangular patch antennas are presented in Figs. 5 and the results for the coaxially-fed circular patch are shown in Fig. 6. The measured results are in very good agreement with the calculated ones, especially for the first three modes. Errors for higher-order modes are due to deviation of the assumed dielectric properties over 8GHz from the real values and also to errors in the effective dimensions of the patch.

The far field can also be predicted from the equivalence-principle surface currents inside the FDTD problem space. The far fields of the coaxially-fed circular patch for two principal planes at its fundamental mode (5.2 GHz) are shown in Figs 7 and 8. For this linearly-polarised field pattern the backlobe was found to be 17dB below the main lobe. The field strength radiating in the nadir direction due to the finite size of the ground plane was found to be 12.5 dB below the maximum, but only about 0.5dB below the zenith value. Variation of the dielectric and ground size from  $46 \times 46$  cells to  $60 \times 60$  cells did not affect the return loss whereas the backlobe intensity varied from 15dB to 20dB below the mainlobe. The zenithal radiation also slightly changed, from 11dB to 14dB below the mainlobe.

#### 4. CONCLUSIONS

An approach to broadband analysis of microstrip patch antennas with finite dielectric and ground planes using FDTD has been presented. As well as avoiding infinite-substrate approximations, the method includes realistic models for stripline and coaxial feeds. Computed values of the return loss were found to be in good agreement with measurements. The return loss was found to be approximately independent of substrate area. Because of the finite substrate, the far fields of the fundamental mode in the nadir direction were found to be almost as strong as those in the zenith direction.

#### REFERENCES

- [1] A. Sommerfeld, 'Partial differential equations in physics', New York: Academic Press, 1964.
- [2] T.K. Sarkar, S. Rao and A.R. Djordjevic, 'Electromagnetic scattering and radiation from finite microstrip structures', IEEE Trans. Microwave Theory and Techniques, Vol. 38, No. 11, pp. 1568-1575, 1990.
- [3] R.A. Abd-Alhameed, N.J. McEwan, P.S. Excell, and M.M. Ibrahim, 'Procedure for analysis of microstrip patch antennas using the method of moments', IEE Proc. Microwaves, Ant and Prop., Vol. 145, No. 6, pp 455-459, 1998.
- [4] A. Taflove, 'Computational electrodynamics: the finite difference time domain method', Boston: Artech House.
- [5] Z.Q. Bi, K.L. Wu, C. Wu and J. Litva, 'Accurate characterisation of planar printed antennas using finite difference time domain method', IEEE Trans. Antennas and Propagation, Vol. 40, No. 5, pp. 526-533, 1992.
- [6] D.M. Sheen, S.M. Ali, M.D. Abouzahara and J.A. Kong, 'Application of the three-dimensional finite difference time domain method to the analysis of planar microstrip circuits', IEEE Trans. MTT, Vol. 38, pp. 849-857, 1989.
- [7] R. Holland and L. Simpson, 'Finite-difference analysis of EMP coupling to thin struts and wires', IEEE Trans. Electromagnetic Compatibility, Vol. EMC-23, No. 2, 1981.
- [8] R.J. Luebbers and H.S. Langdon, 'A simple feed model that reduces time steps needed for FDTD antenna and microstrip calculations', IEEE Trans. Antennas and Propagation, Vol. 44, No. 7, pp. 1000-1005, 1996.
- [9] J.G. Maloney, G.S. Smith and W.R. Scott, 'Accurate computation of the radiation from simple antennas using the finite difference time domain method', IEEE Trans. Antennas and Propag., Vol. 38, pp. 1059-1068, 1990.
- [10] K.L. Wu, M. Spenuk, J. Litva and D.G. Fang, 'Theoretical and experimental study of feed network effects on the radiation pattern of series-fed microstrip antenna arrays', IEE Proc., Pt. H, Vol. 138, pp. 238-242, 1991.

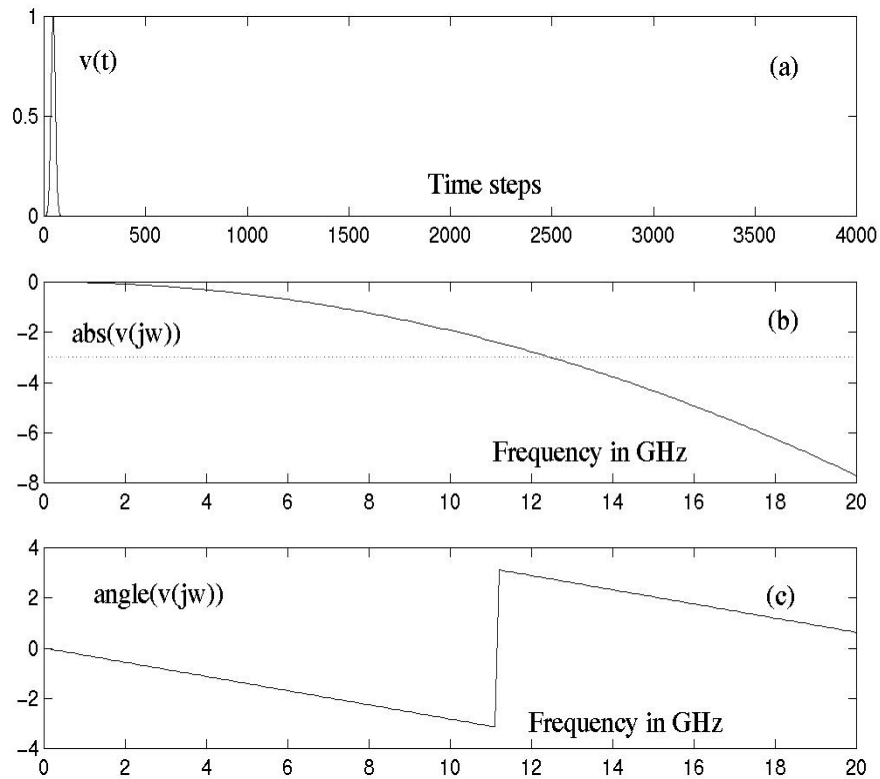


**Fig. 1.** Characteristics of the Gaussian pulse: a) as a function of time steps, b) and c) are the magnitude and phase of the spectrum respectively.

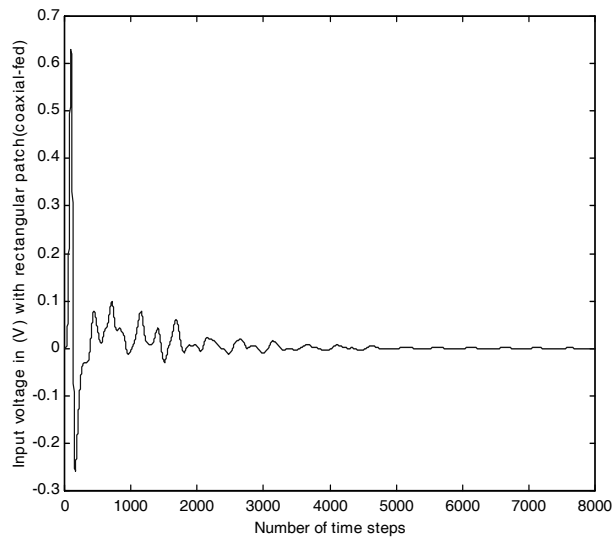


**Fig. 2.** The input voltage at the input port of the coaxially-fed rectangular patch antenna.

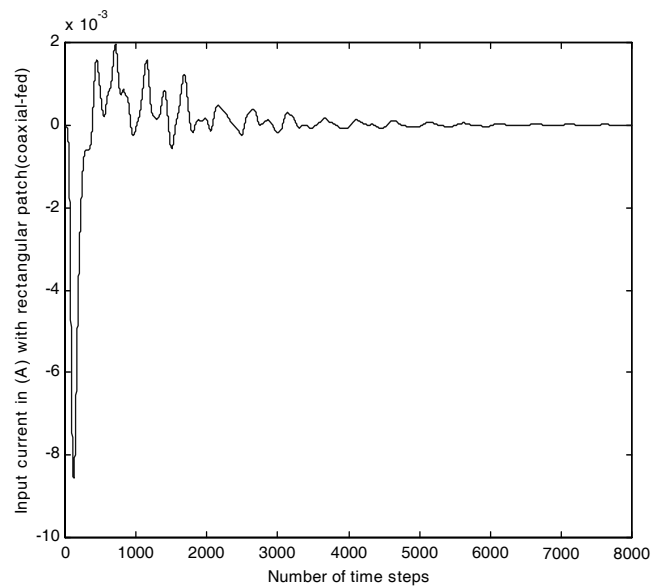
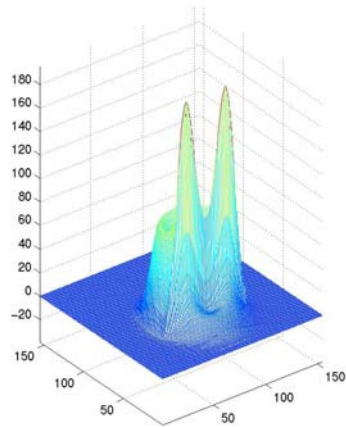
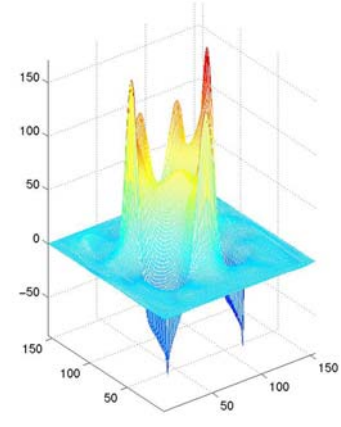


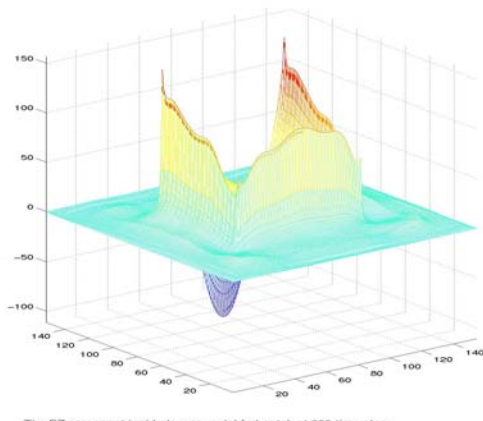
**Fig. 3** The input current at the input port of the coaxially-fed rectangular patch antenna.



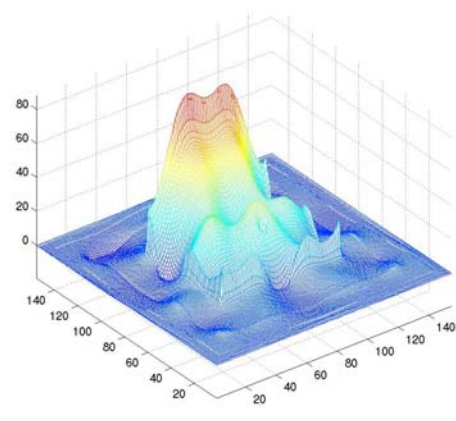
(a) 200 time steps



(b) 400 time steps



(c) 600 time steps



(d) 800 time steps

**Fig. 4** The  $E_z$  component just below the coaxial line fed rectangular patch antenna.

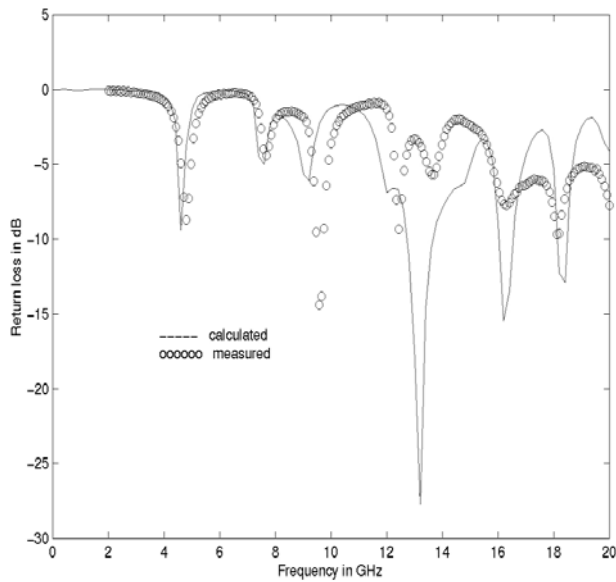


**Fig. 5.** Return loss for stripline-fed rectangular patch.

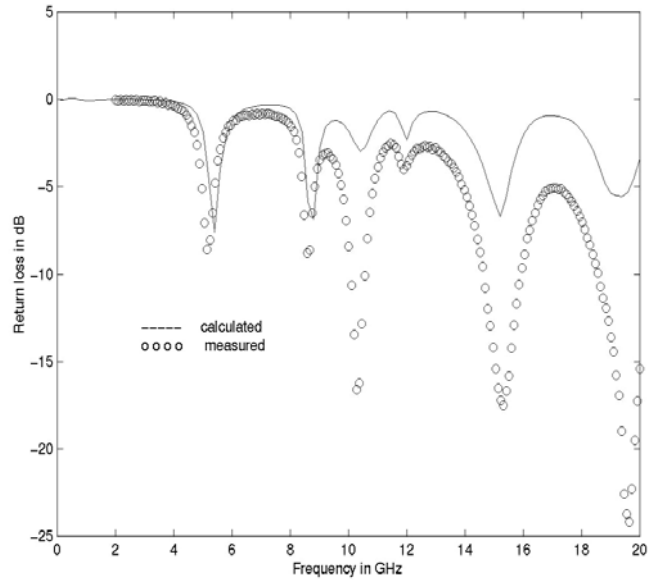


**Fig. 6.** Return loss for coaxially-fed circular patch.

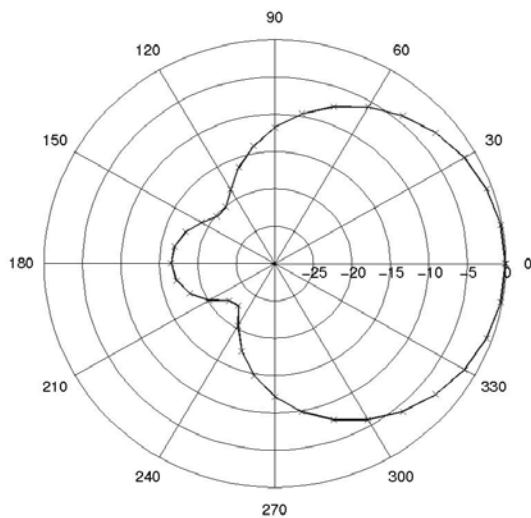


**Fig. 7**  $E_\theta$  versus  $\theta$  at  $\phi = 90^\circ$  for the fundamental mode (5.2GHz) of the coaxially-fed circular patch antenna.

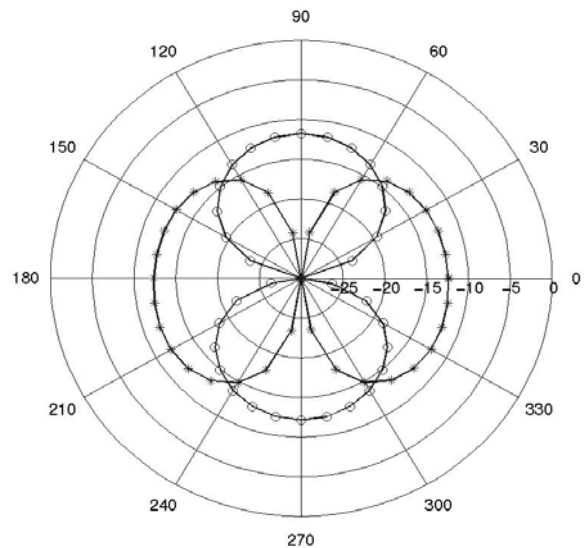


**Fig. 8.**  $E_\theta$  (\*\*\*) and  $E_\phi$  (ooo) versus  $\phi$  at  $\theta = 90^\circ$  for the fundamental mode (5.2GHz) of the coaxially-fed circular patch antenna.